

# Tissue-specific transplantation antigen P35B functions as an oncogene and is regulated by microRNA-125a-5p in lung cancer

YINGJIE GAO<sup>1</sup>, GUANGLIANG ZHANG<sup>1</sup>, JINLONG LIU<sup>2</sup> and HUIMIN LI<sup>1</sup>

Departments of <sup>1</sup>Oncology and <sup>2</sup>Orthopedics, Liaocheng People's Hospital, Liaocheng, Shandong 252000, P.R. China

Received January 15, 2020; Accepted September 16, 2020

DOI: 10.3892/or.2021.8023

**Abstract.** Tissue-specific transplantation antigen P35B (TSTA3) expression is upregulated in esophageal squamous cell carcinoma and breast cancer, and functions as an oncogene in breast cancer. However, the roles and underlying mechanisms of TSTA3 in lung cancer have not been fully elucidated. The current study aimed to reveal the role of TSTA3 in lung cancer and explore whether TSTA3 may be modulated by microRNA (miR)-125a-5p to activate  $\beta$ -catenin signaling. Immunohistochemical staining and western blotting were used to analyze TSTA3 expression in lung cancer tissues and cells. Cell functions were assessed via Cell Counting Kit-8, flow cytometry, wound-healing, Transwell and *in vivo* tumor formation assays. The effect of TSTA3 on the activation of  $\beta$ -catenin signaling was determined using western blot and immunofluorescence analyses. The association between miR-125a-5p and TSTA3 was determined by western blotting and luciferase gene reporter assay. The present study revealed that, compared with normal tissues and cells, TSTA3 expression was significantly increased in lung cancer tissues and cell lines, and high TSTA3 expression predicted a poor prognosis and more malignant clinical features in patients with lung cancer. TSTA3 upregulation significantly enhanced  $\beta$ -catenin expression and promoted its nuclear accumulation. In addition, TSTA3 expression was negatively regulated by miR-125a-5p, which was downregulated in lung cancer. Furthermore, TSTA3 overexpression markedly promoted cell proliferation, migration, invasion and tumorigenesis, and suppressed cell apoptosis. TSTA3 downregulation abolished the effects of miR-125a-5p downregulation on promoting lung cancer cell malignant transformation. Overall, the current study demonstrates that TSTA3 is regulated by miR-125a-5p and functions as an oncogene in lung cancer via promoting the activation of  $\beta$ -catenin signaling.

## Introduction

Lung cancer is one of the leading causes of cancer-associated deaths in the world, with ~1.5 million new cases diagnosed annually worldwide (1,2). In 2008, ~1.4 million people died from lung cancer, accounting for 18% of all cancer-associated mortalities (2). Non-small cell lung cancer (NSCLC), accounting for 70-80% of all lung cancer cases, is the main sub-type of lung cancer (3). Despite progress being made in the treatment means, such as surgical resection, adjuvant radiotherapy and chemotherapy, the prognosis in patients with lung cancer has not been markedly improved over the years (4). The conversion of cells into a metastatic phenotype contributes to the majority ( $\geq 90\%$ ) of cancer deaths (5). Therefore, it is essential to further elucidate the molecular mechanisms underlying the occurrence and development of lung cancer.

Tissue-specific transplantation antigen P35B (TSTA3), also known as GDP-D-mannose-4,6-dehydratase or GDP-4-keto-6-deoxy-D-mannose-3,5-epimerase-4-reductase, is located on chromosome 8q24.3 and is responsible for the conversion of cellular GDP-D-mannose into GDP-L-fucose, which is the substrate of several kinds of fucosyltransferases (6). Increasing evidence has indicated that the dysregulation of GDP-L-fucose serves a crucial role in promoting cancer cell metastasis and invasion in various types of cancer, such as hepatocellular carcinoma and colorectal cancer (7,8), suggesting that TSTA3 may be involved in carcinogenesis. Subsequent studies have confirmed the vital role of TSTA3 in the progression of cancer. For example, Yang *et al* (9) reported that TSTA3 expression is frequently upregulated in esophageal squamous cell carcinoma (ESCC), and its high expression levels are closely associated with a poor prognosis in patients with ESCC. Similarly, Sun *et al* (10) demonstrated that TSTA3 expression is upregulated in breast cancer tissues and cells, and is closely associated with poor survival rates and advanced clinical progression of breast cancer cases. Additionally, downregulation of TSTA3 using small interfering RNA transfection significantly weakens the cell invasive and proliferative capacities, suggesting that TSTA3 functions as an oncogene in breast cancer (10). In lung cancer, Rotunno *et al* (11) revealed that TSTA3 expression is significantly elevated in lung adenocarcinoma tissues compared with in normal tissues using genome-wide mRNA expression analysis. However, the roles and underlying mechanisms of TSTA3 in lung cancer progression remain unclear.

**Correspondence to:** Dr Huimin Li, Department of Oncology, Liaocheng People's Hospital, 67 Dongchang West Road, Liaocheng, Shandong 252000, P.R. China  
E-mail: jys1124@163.com

**Key words:** lung cancer, tissue-specific transplantation antigen P35B, microRNA-125a-5p,  $\beta$ -catenin

MicroRNAs (miRNAs/miRs) are a class of endogenous non-coding RNAs of 21-24 nucleotides in length derived from pri- and pre-miRNAs (12,13). miRNAs, as post-transcriptional regulators, induce translational repression of target genes via partial complementarity to specific sequences of their 3'-untranslated region (UTR) (14). miR-125a-5p has been identified as an upstream miRNA of TSTA3 in breast cancer (10). It has been reported that miR-125a-5p expression is downregulated in lung cancer and serves as a tumor suppressive gene (15,16), but whether miR-125a-5p regulates TSTA3 expression and is involved in lung cancer progression remains unknown.

The hyperactivation of the Wnt/ $\beta$ -catenin signaling pathway serves vital roles in lung cancer progression (17).  $\beta$ -catenin acts as a component of cell-cell adhesion structure via interacting with the cytoplasmic domain of E-cadherin, as well as a cellular signaling molecule following the activation of the Wnt signaling pathway (18). In the absence of Wnt, the  $\beta$ -catenin protein is restrained in the cytoplasm at a low level, where it will be degraded by a protein complex consisting of axis inhibitor (Axin), adenomatous polyposis coil (APC), casein kinase 1 (CK1) and glycogen synthase kinase 3 $\beta$  (GSK-3 $\beta$ ) via the ubiquitin-proteasome pathway (19). During this process,  $\beta$ -catenin is first phosphorylated at Ser45 by CK1, leading to the subsequent phosphorylation of  $\beta$ -catenin by GSK-3 $\beta$ , which destabilizes  $\beta$ -catenin by phosphorylating it at Ser33, Ser37 and Thr41 (20).  $\beta$ -catenin accumulates in the cytoplasm and translocates to the nucleus when Wnt signaling is activated, leading to the transcription of target genes, such as c-Myc and cyclin D1, via interacting with the T-cell factor/lymphoid enhancer factor family (21,22). It has been demonstrated that targeting the Wnt/ $\beta$ -catenin signaling pathway is a promising method for the treatment of cancer, including lung cancer (23).

The present study focused on exploring the roles and molecular mechanisms of TSTA3 in lung cancer progression.

## Materials and methods

**miRNA target prediction.** The miRNA targets predicted using publicly available algorithms were obtained from TargetScan 7.2 (<http://www.targetscan.org>) and miRDB (<http://www.mirdb.org/miRDB/>). Putative target genes predicted by three algorithms were selected as candidates.

**Tissue samples.** A total of 88 pairs of primary lung cancer tissues and their corresponding adjacent normal lung tissues ( $\geq 5$  cm from the carcinoma) were obtained from patients with lung carcinoma who underwent excision surgery between June 2016 and December 2018. Among them, 60 cases were diagnosed with NSCLC and 28 cases with small cell lung cancer. Patients had a mean age of  $61.8 \pm 13.4$  years (range, 47-72 years). Informed consent forms were signed by all patients. The TNM stage was evaluated based on the staging system provided by the International Association for the Study of Lung Cancer (24). The present study involving human samples was performed in accordance with the Declaration of Helsinki and was approved by the Ethics Committee of Liaocheng People's Hospital (Liaocheng, China).

**Immunohistochemical staining (IHC).** The tissues were fixed in 10% neutral formalin for 2 days at room temperature,

embedded in paraffin and cut into 4- $\mu$ m-thick sections. Subsequently, the sections were deparaffinized in xylene and rehydrated in a graded alcohol series, followed by antigen retrieval with sodium citrate (pH 6.7) in a pressure-cooker for 30 min and blocking with 5% goat serum (Beijing Solarbio Science & Technology Co., Ltd.) for 1 h at room temperature. Subsequently, sections were incubated with a primary anti-TSTA3 antibody (1:200; cat. no. ab190002; Abcam) overnight at 4°C, and probed with a HRP-conjugated secondary antibody (40-120  $\mu$ l; cat. no. 8114; Cell Signaling Technology, Inc.) for 1 h at room temperature. Sections were then incubated with chromogen 3,3'-DAB (R&D Systems, Inc.) for 30 sec at room temperature. Cell nuclei were stained with Harris' hematoxylin solution for 2 min at room temperature. The staining was assessed using a light microscope at a magnification of  $\times 100$ .

The expression levels of TSTA3 in lung cancer and normal tissues were assessed according to the staining extent and intensity as previously reported (24). The staining extent was scored according to the percentage of positively stained cells: 0,  $<5\%$ ; 1, 5-25%; 2, 26-50%; 3, 51-75%; and 4,  $>75\%$ . The staining intensity was scored as follows: 0, Negative (no staining); 1, mild (weak staining; light brown color); 2, intermediate (moderate staining; brown color); and 3, intense (strong staining; dark brown color). The scores of staining intensity and staining extent were multiplied to obtain a total score up to 12. The scoring was determined by three independent evaluators who were blinded to the clinicopathological characteristics of the patients. Patients with a total TSTA3 score higher than the median score (score=6) were considered as the high expression group, while patients with a score lower than the median score represented the low expression group.

**Cell lines and culture conditions.** The human bronchial epithelial BESA-2B cell line, and lung cancer A549 (human NSCLC), NCI-H1299 (human NSCLC) and NCI-H446 (human small cell lung cancer) cell lines were all purchased from the American Type Culture Collection.

BEAS-2B cells were maintained in high glucose DMEM supplemented with 10% FBS. NCI-H1299 and NCI-H446 cells were grown in RPMI-1640 medium, and A549 cells were cultured in F-12K medium, all supplemented with 10% FBS. All cells were maintained at 37°C with 5% CO<sub>2</sub>. All reagents were purchased from Thermo Fisher Scientific, Inc.

**Cell transfection.** Three TSTA3 short hairpin (sh)RNAs (sh-TSTA3), TSTA3 lentiviral overexpression vector (OE-TSTA3), miR-125a-5p inhibitors, mimics and the non-targeting scrambled negative controls (NCs) were all purchased from Shanghai GenePharma Co., Ltd. Lung cancer cells ( $1 \times 10^5$  cells/well) were seeded in 6-well plates and incubated at 37°C overnight, followed by lentiviral transfection using polybrene (Hanbio Biotechnology Co., Ltd.) with a multiplicity of infection of 4 for sh-TSTA3 and 6 for OE-TSTA3. miR-125a-5p inhibitors (100 nM), mimics (40 nM), inhibitor-NC (100 nM) and mimics-NC (40 nM) were transfected into cells using Lipofectamine<sup>®</sup> 3000 (Thermo Fisher Scientific, Inc.) according to the manufacturer's protocol. To establish stable cell lines, the transfected cells were incubated with 4  $\mu$ g/ml puromycin (Beijing Solarbio Science & Technology Co., Ltd.)

Table I. Primer sequences.

| Gene             | Sequences (5'-3') |   |
|------------------|-------------------|---|
| TSTA3            | Sense:            | GGATGCTCCGTGCAACTG                                  |
|                  | Antisense:        | CGGGTAGGTCGTCTTGTCTAG                               |
| APC              | Sense:            | AGACAGAATGGAGGTGCTGC                                |
|                  | Antisense:        | ACCGCAGTTTTACTCCAGGG                                |
| Axin             | Sense:            | GGATGAGGACGATGGCAGAG                                |
|                  | Antisense:        | GGAATGTGAGGTAGGGGCAC                                |
| GSK-3 $\beta$    | Sense:            | GGACTAAGGTCTTCCGACCC                                |
|                  | Antisense:        | TTAGCATCTGACGCTGCTGT                                |
| CK1 $\alpha$     | Sense:            | CCCGAGATCCCTTTCCACAGA                               |
|                  | Antisense:        | CCAACACAAAATGCCCCCAG                                |
| $\beta$ -catenin | Sense:            | GCGCCATTTTAAGCCTCTCG                                |
|                  | Antisense:        | GGCCATGTCCAACCTCCATCA                               |
| GAPDH            | Sense:            | CCACTAGGCGCTCACTGTTCT                               |
|                  | Antisense:        | GCATCGCCCCACTTGATTTT                                |
| miR-125a-3p      | Sense:            | ACACTCCAGCTGGGACAGGTG<br>AGGTTCTTG                  |
|                  | Antisense:        | CTCAACTGGTGTCTGGAGTC<br>GGCAATTCAGTTGAGG<br>GCTCCCA |
| U6               | Sense:            | CTCGCTTCGGCAGCACA                                   |
|                  | Antisense:        | AACGCTTCACGAATTTGCGT                                |

TSTA3, tissue-specific transplantation antigen P35B; Axin, axis inhibitor; APC, adenomatous polyposis coil; CK1, casein kinase 1; GSK-3 $\beta$ , glycogen synthase kinase 3 $\beta$ ; miR, microRNA.

and/or 100  $\mu$ g/ml G418 (Beijing Solarbio Science & Technology Co., Ltd.) for a total of 14 days at 37°C. Following 48 h of transfection, cells were collected for subsequent experiments. The sequences were as follows: Mimic-miR-125a-5p, 5'-uccugagaccuuuaaccuguga-3'; mimic-NC, 5'-uucuccgaacugucacgutt-3'; inhibitor-miR-125a-5p, 5'-agggaacucugggaaauuggacacu-3'; and inhibitor-NC, 5'-caguacuuuuguguaguacaa-3'.

**RNA preparation and reverse transcription-quantitative PCR (RT-qPCR).** After total RNA extraction from cells using TRIzol® reagent (Thermo Fisher Scientific, Inc.), the TaqMan Reverse Transcription kit (Takara Biotechnology Co., Ltd.) was used to obtain cDNA for mRNA detection (42°C for 1 h), while TaqMan MicroRNA Reverse Transcription kit (Takara Biotechnology Co., Ltd.) was used for miRNA detection (42°C for 1 h). Subsequently, RT-qPCR was performed to assess the expression levels of miR-125a-5p using specific primers with U6 as a control. GAPDH expression was used to normalize the expression levels of mRNAs. RT-qPCR was performed with SYBRGreen (Thermo Fisher Scientific, Inc.) on the ABI 7500 Sequence Detection System (Thermo Fisher Scientific, Inc.). Reaction conditions were as follows: 94°C for 5 min, followed by amplification for 40 cycles at 94°C for 30 sec, 57°C for 30 sec and 72°C for 30 sec, and a final step at 72°C for 5 min. The expression levels of miR-125a-5p and mRNAs were calculated using the  $2^{-\Delta\Delta C_q}$  method (25). The primer sequences

used in the present study are listed in Table I. Patients with miR-125a-5p expression higher than the median expression were considered as the high expression group, while those with lower expression were considered as the low expression group.

**Western blotting.** Total protein was extracted from tissues and cells using RIPA lysis buffer [Roche Diagnostics (Shanghai) Co., Ltd.] supplemented with 1% protease inhibitor (Beijing Solarbio Science & Technology Co., Ltd.). After centrifugation at 12,000  $\times$  g at 4°C for 25 min, protein concentration was determined using a BCA Protein assay kit (Thermo Fisher Scientific, Inc.) according to the manufacturer's protocol. Subsequently, protein samples (25  $\mu$ g protein/lane) were separated via 10% SDS-PAGE and transferred to polyvinylidene difluoride membranes (EMD Millipore). After incubation with 5% skimmed milk for 1 h at room temperature, the membranes were probed overnight at 4°C with the following primary antibodies against: TSTA3 (cat. no. ab190002; Abcam),  $\beta$ -catenin (cat. no. ab16051; Abcam), phospho (p)- $\beta$ -catenin (Ser33; cat. no. PA5-37543; Thermo Fisher Scientific, Inc.), APC (cat. no. ab15270; Abcam), GSK-3 $\beta$  (cat. no. ab32391; Abcam), Axin (cat. no. ab32197; Abcam) and CK1 (cat. no. 2655; Cell Signaling Technology, Inc.), all at 1:2,000 dilution. Subsequently, the membranes were incubated with HRP-conjugated secondary antibodies (1:10,000; cat. nos. SA00001-1 and SA00001-2; ProteinTech Group, Inc.) for 1 h at room temperature. After washing three times with PBS, protein signaling was enhanced using an ECL reagent (EMD Millipore) and detected on ProfiBlot-48 (Tecan Group, Ltd.). The gray-scale value analysis was performed using ImageJ software (version 1.48; National Institutes of Health).

**Luciferase gene reporter assay.** The wild-type (WT) or mutant (MT) of luciferase (Luc)-TSTA3-3'-UTR vectors were obtained from Shanghai GenePharma Co., Ltd. NCI-H1299 cells were plated into 96-well plates at 60% confluence and incubated at 37°C overnight, followed by cell co-transfection with WT or MT vector and miR-125a-5p inhibitors (100 nM), mimics (40 nM), inhibitor-NC (100 nM) or mimic-NC (40 nM), or *Renilla* luciferase vector (used as a control) using Lipofectamine 3000. After 48 h of transfection, the firefly and *Renilla* luciferase fluorescence values were detected using a Dual-Luciferase Reporter System (Promega Corporation). The ratio of firefly luciferase activity to *Renilla* luciferase activity was used to indicate the relative luciferase activity.

**Cell Counting Kit-8 (CCK-8) assay.** Lung cancer cells were harvested and seeded in 96-well plates at a density of 3,000 cells/well and cultured for 24, 48, 72 or 96 h at 37°C. Subsequently, 10  $\mu$ l CCK-8 solution (MedChemExpress) was added into each well, followed by incubation for another 4 h at 37°C according to the manufacturer's protocol. The absorbance was measured at 450 nm using a microplate reader (BioTek Instruments, Inc.).

**Clone formation assay.** The stable cell lines were harvested and added into 6-well plates at a density of 100 cells/well. Following incubation at 37°C for 14 days, the cells were washed with PBS, fixed with methanol for 10 min and stained with 0.1% crystal violet solution (Beijing Solarbio Science & Technology

Co., Ltd.) for 20 min both at room temperature. The visible colonies were counted manually after the cells were washed with PBS for several times.

**Flow cytometry analysis.** After 48 h of cell transfection, lung cancer cells were harvested and stained with Annexin V (FITC) and propidium iodide (PI) reagent (Dojindo Molecular Technologies, Inc.) for 15 min at room temperature, according to the manufacturer's protocol. Cell apoptosis rates were detected via flow cytometry using CytoFLEX (Beckman Coulter, Inc.) and analyzed using FlowJo 7.6 software (FlowJo LLC). The apoptotic cells represent both Annexin V<sup>+</sup>/PI<sup>-</sup> (early apoptotic) cells and Annexin V<sup>+</sup>/PI<sup>+</sup> (late apoptotic) cells.

**Wound-healing assay.** For wound-healing assays, the transfected lung cancer cells were cultured in their respective medium in a 6-well plate until they reached 100% confluence. Subsequently, wounds were made using 20- $\mu$ l tips and the medium was replaced with serum-free medium. After 24 h of incubation at 37°C, the width of the wounds was observed and recorded using an inverted light microscope (magnification, x40). Cell migration ability was quantified using the ratio of the wound area at 24 h to the wound area at 0 h.

**Transwell assay.** Cell invasive capacity was determined using Transwell chambers coated with Matrigel<sup>®</sup> (8  $\mu$ m; BD Pharmingen; BD Biosciences). Lung cancer cells were seeded in the upper chambers at a concentration of  $1 \times 10^5$  cells/well in their respective serum-free medium, while 600  $\mu$ l of the respective medium containing 10% FBS was added in the lower chambers. After 48 h of incubation at 37°C, cells in the upper chambers were removed using cotton swabs, and the invaded cells in the lower chambers were stained with 0.1% crystal violet for 10 min at room temperature. Cell invasive ability was assessed by manually counting the total number of invaded cells under an optical light microscope at a magnification of x100.

**Immunofluorescence.** After 24 h of cell transfection, NCI-H1299 cells were harvested and seeded onto glass cover slips in a 24-well plate and cultured for 48 h at 37°C. Subsequently, the cells were fixed with 4% paraformaldehyde for 15 min at room temperature and then stained with a rabbit polyclonal  $\beta$ -catenin antibody (1:100; cat. no. ab16051; Abcam) at 4°C overnight, followed by incubation with the Texas Red-X-conjugated fluorescent secondary antibody (1:2,000; cat. no. T-6391; Invitrogen; Thermo Fisher Scientific, Inc.) for 45 min at room temperature. Nuclei were stained with DAPI (Beyotime Institute of Biotechnology) at a dilution of 1:10,000 for 5 min at room temperature. The glass cover slips were covered with VECTASHIELD antifade mounting medium (Vector Laboratories, Inc.). The expression levels and location of  $\beta$ -catenin were detected using a laser scanning fluorescence microscope (TCSSP2-AOBS-MP; Leica Microsystems, Inc.) at a magnification of x100.

**Mice tumor-bearing experiment.** A total of 20 male, 4-6 weeks old, BALB/c nude mice (20-25 g) were purchased from Beijing Vital River Laboratory Animal Technology Co., Ltd., and used for tumor-bearing experiments. All mice were housed in a specific pathogen-free animal facility with free

access to water and food at 22 $\pm$ 1°C with 55 $\pm$ 2% humidity and a 12 h light/dark cycle. Experimental protocols involving animals were approved by the Ethics Committee of Liaocheng People's Hospital.

**Mice were subcutaneously injected in the armpit area with stably transfected NCI-H1299 cells ( $1 \times 10^7$  cells diluted in 200  $\mu$ l PBS).** Each group (control, OE-TSTA3, inhibitors, inhibitors+sh-TSTA3) contained 5 mice. At 28 days post-injection, the tumours were removed and weighed unless the tumour diameter reached 1.8 cm, at which point the mice would be sacrificed early. The animal health and behaviour were monitored every 3 days. The mice were euthanized by cervical dislocation. The largest tumour volume was  $\sim 1.4$  cm<sup>3</sup> and the largest tumour diameter was  $\sim 1.2$  cm.

**Statistical analysis.** Data from three independent experiments were expressed as the mean  $\pm$  SD. Statistical analyses were performed using SPSS 21.0 software (IBM Corp.). The difference between the staining scores of two groups was analyzed using Wilcoxon signed rank test. The association between TSTA3 expression levels and the clinicopathological features of patients with lung cancer was analyzed using  $\chi^2$  test. Kaplan-Meier curves with log-rank tests were used to assess the association between TSTA3 expression and overall survival. Comparisons between 2 groups or among multiple groups were determined via paired Student's t-test for comparisons between tumor and para-carcinoma normal tissues, and unpaired Student's t-test for other comparisons, or one way ANOVA followed by Bonferroni post hoc test, respectively.  $P < 0.05$  was considered to indicate a statistically significant difference.

## Results

**TSTA3 expression is upregulated in lung cancer tissues and cells.** To explore the effects of TSTA3 in the progression of lung cancer, its expression pattern was determined in lung cancer tissues and cell lines. The IHC staining for TSTA3 (Fig. 1A and B) in tumor tissues was significantly enhanced compared with that in the para-carcinoma normal tissues. Consistently, the western blotting (Fig. 1C) results revealed that TSTA3 expression was significantly increased in representative lung cancer tissues compared with that in normal tissues (Fig. 1B and C). In addition, TSTA3 expression in lung cancer cell lines, including A549, NCI-H1299 and NCI-H446 cells, was significantly increased compared with that in normal lung BEAS-2B cells (Fig. 1D). The present results revealed that TSTA3 was highly expressed in lung cancer.

**High TSTA3 expression is associated with advanced clinical features and poor prognosis in patients with lung cancer.** Subsequently, the association between TSTA3 expression and the clinical features and prognosis in patients with lung cancer was investigated. As shown in Table II, patients with high TSTA3 expression were inclined to poor/moderate differentiation ( $P = 0.027$ ) and high incidence of lymph node metastasis ( $P = 0.011$ ), as well as an advanced stage ( $P = 0.016$ ). Furthermore, patients with high TSTA3 expression ( $n = 49$ ) had

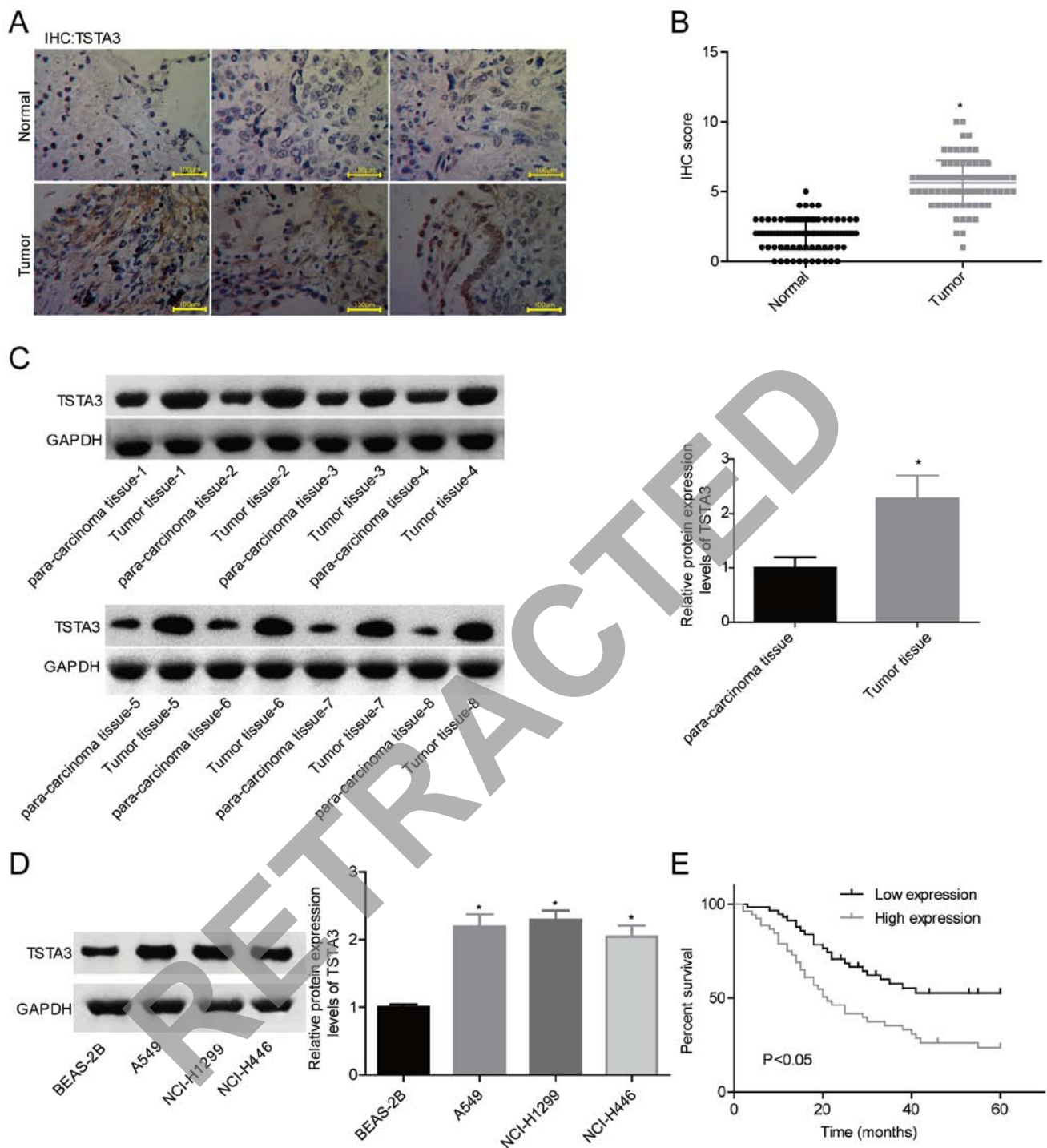


Figure 1. Assessment of TSTA3 expression and clinical value in lung cancer. The protein expression levels of TSTA3 in lung cancer and normal tissues were determined by (A and B) IHC (scale bar, 100  $\mu$ m) and (C) western blotting. \*P<0.05 vs. normal/para-carcinoma tissues. (D) Western blot analysis of the protein expression levels of TSTA3 in lung cancer cell lines including A549, NCI-H1299 and NCI-H446, and normal lung BEAS-2B cells. \*P<0.05 vs. BEAS-2B. (E) Kaplan-Meier analysis was used to compare the overall survival of patients with lung cancer with high (n=49) or low (n=39) TSTA3 expression. IHC, immunohistochemistry; TSTA3, tissue-specific transplantation antigen P35B.

a shorter overall survival time than patients with low TSTA3 expression (n=39) (Fig. 1E). These results demonstrated that high TSTA3 expression was associated with the malignant clinical progress and poor prognosis in patients with lung cancer.

*TSTA3 accelerates the malignant phenotypic transformation of lung cancer cells.* To explore the function of TSTA3 in the

progression of lung cancer, gain- and loss-of-function assays were performed. Among the 3 shRNAs targeting the human TSTA3 gene, sh-1 exhibited the highest knockdown efficiency and was therefore used in subsequent experiments, while OE-TSTA3 significantly promoted TSTA3 expression at the mRNA (Fig. 2A) and protein (Fig. 2B) levels in NCI-H1299 cells. Ectopic TSTA3 expression in NCI-H1299 cell clone OE-TSTA3 transfection significantly increased cell clone

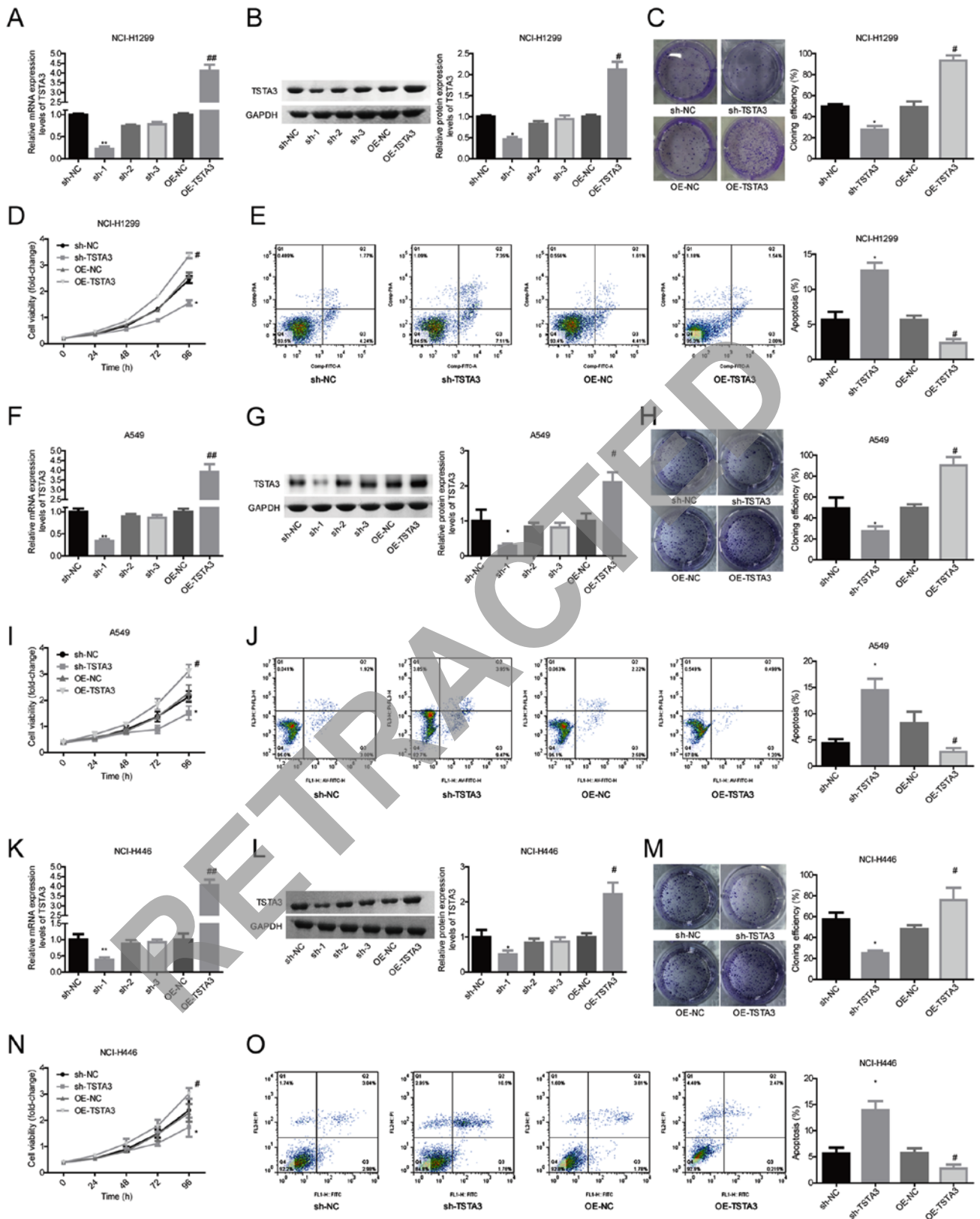


Figure 2. Evaluation of TSTA3 role in cell proliferation, clone formation and apoptosis. NCI-H1299 cells were transfected with OE-NC, OE-TSTA3, sh-NC or sh-TSTA3, and then the expression levels of TSTA3 at the (A) mRNA and (B) protein levels were determined via western blotting and RT-qPCR. (C) Clone formation ability was assessed via clone formation assay. (D) Cell proliferation was determined via CCK-8 assay. (E) Cell apoptosis was assessed via flow cytometry. A549 cells were transfected with OE-NC, OE-TSTA3, sh-NC or sh-TSTA3, and then the expression levels of TSTA3 at the (F) mRNA and (G) protein levels were determined via western blotting and RT-qPCR. (H) Clone formation ability was assessed via clone formation assay. (I) Cell proliferation was determined via CCK-8 assay. (J) Cell apoptosis was assessed via flow cytometry. NCI-H446 cells were transfected with OE-NC, OE-TSTA3, sh-NC or sh-TSTA3, and then the expression levels of TSTA3 at the (K) mRNA and (L) protein levels were determined via western blotting and RT-qPCR. (M) Clone formation ability was assessed via clone formation assay. (N) Cell proliferation was determined via CCK-8 assay. (O) Cell apoptosis was assessed via flow cytometry. \* $P < 0.05$  vs. sh-NC; # $P < 0.05$ , ## $P < 0.01$  vs. OE-NC. NC, negative control; OE, overexpressed; sh, short hairpin; RT-qPCR, reverse transcription-quantitative PCR; TSTA3, tissue-specific transplantation antigen P35B; CCK-8, Cell Counting Kit-8.

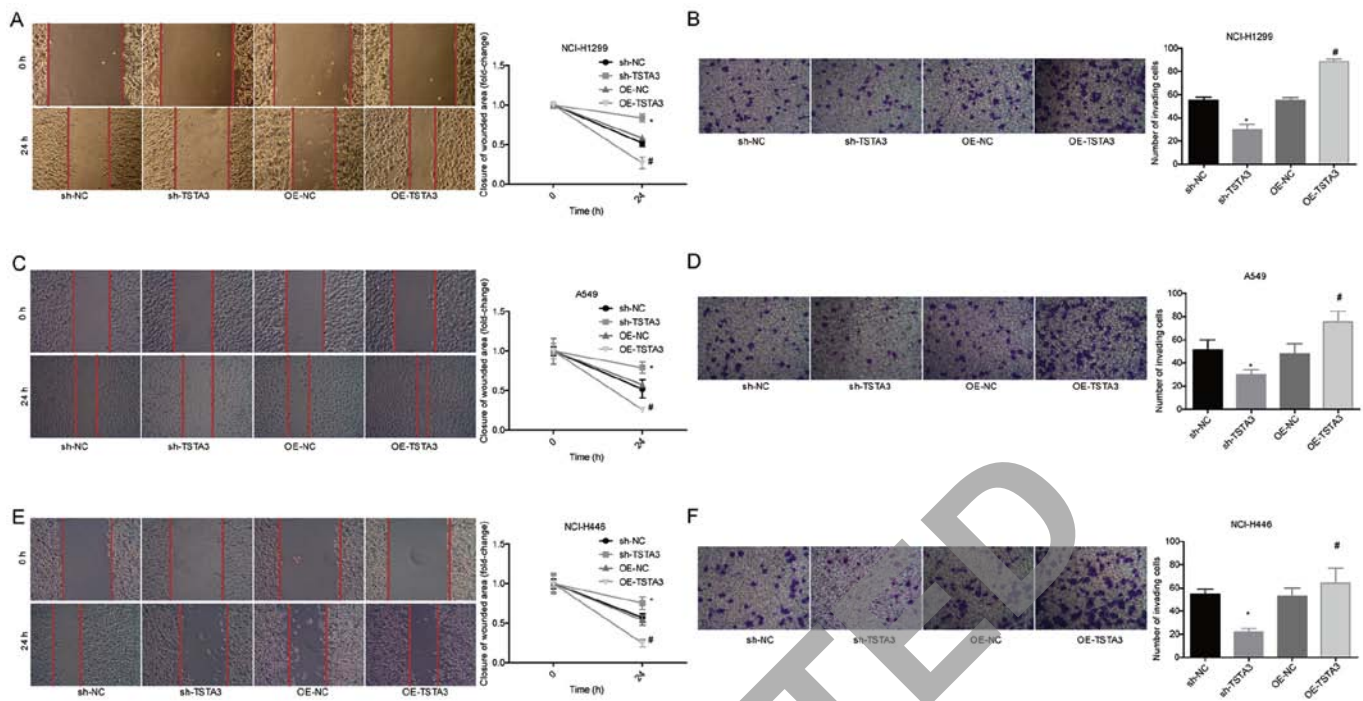


Figure 3. Role of TSTA3 in migration and invasion of lung cancer cells. NCI-H1299 cells were transfected with OE-NC, OE-TSTA3, sh-NC or sh-TSTA3, and then analyzed via (A) wound-healing and (B) Transwell invasion assays. A549 cells were transfected with OE-NC, OE-TSTA3, sh-NC or sh-TSTA3, and then analyzed via (C) wound-healing and (D) Transwell invasion assays. NCI-H446 cells were transfected with OE-NC, OE-TSTA3, sh-NC or sh-TSTA3, and then analyzed via (E) wound-healing (magnification, x50) and (F) Transwell invasion assays (magnification, x100). \* $P < 0.05$  vs. sh-NC; # $P < 0.05$  vs. OE-NC. NC, negative control; OE, overexpressed; sh, short hairpin RNA; TSTA3, tissue-specific transplantation antigen P35B.

Table II. Association between TSTA3 expression and the clinical features of patients with lung cancer.

| Variable                | TSTA3 expression |            | P-value |
|-------------------------|------------------|------------|---------|
|                         | High (n=49)      | Low (n=39) |         |
| Sex                     |                  |            | 0.664   |
| Male                    | 27               | 24         |         |
| Female                  | 22               | 15         |         |
| Age, years              |                  |            | 0.133   |
| <60                     | 29               | 16         |         |
| ≥60                     | 20               | 23         |         |
| Histological type       |                  |            | 0.668   |
| Squamous cell carcinoma | 23               | 21         |         |
| Adenocarcinoma          | 26               | 18         |         |
| Differentiation         |                  |            | 0.027   |
| Poor                    | 19               | 8          |         |
| Moderate                | 20               | 13         |         |
| Well                    | 10               | 18         |         |
| Lymph node metastasis   |                  |            | 0.011   |
| No                      | 19               | 26         |         |
| Yes                     | 30               | 13         |         |
| TNM stage               |                  |            | 0.016   |
| I                       | 8                | 13         |         |
| II                      | 11               | 14         |         |
| III                     | 30               | 12         |         |

TSTA3, tissue-specific transplantation antigen P35B.

formation (Fig. 2C) and proliferation (Fig. 2D), and inhibited cell apoptosis (Fig. 2E) compared with the control. On the other hand, knockdown of TSTA3 significantly repressed cell proliferation and clone formation (Fig. 2C and D), and increased cell apoptosis (Fig. 2E) compared with the control. Similar effects of TSTA3 knockdown or overexpression on cell clone formation, proliferation and apoptosis were also observed in A549 (Fig. 2F-J) and NCI-H446 (Fig. 2K-O) cell lines.

Furthermore, cell migration (Fig. 3A, C and E) and invasion (Fig. 3B, D and F) were significantly enhanced when TSTA3 was overexpressed, while knockdown of TSTA3 with sh-TSTA3 transfection significantly inhibited cell migration and invasion in NCI-H1299, A549 and NCI-H446 cells (Fig. 3A-F). These *in vitro* experiment results revealed that TSTA3 may function as an oncogene in lung cancer.

*Overexpression of TSTA3 increases the expression levels and nuclear accumulation of  $\beta$ -catenin in lung cancer cells.* To explore whether the Wnt/ $\beta$ -catenin signaling pathway was involved in TSTA3-mediated lung cancer progression, the effects of TSTA3 on the expression levels of key proteins in the Wnt/ $\beta$ -catenin signaling pathway were explored. Since TSTA3 exhibited similar effects on the viability, apoptosis, migration and invasion of NCI-H1299, A549 and NCI-H446 cells, NCI-H1299 cells were used for representation in subsequent experiments. The western blotting results revealed that  $\beta$ -catenin expression was significantly increased when NCI-H1299 cells were transfected with OE-TSTA3, whereas the expression levels of APC, Axin, GSK-3 $\beta$  and CK1 exhibited no marked change at the protein (Fig. 4A) and

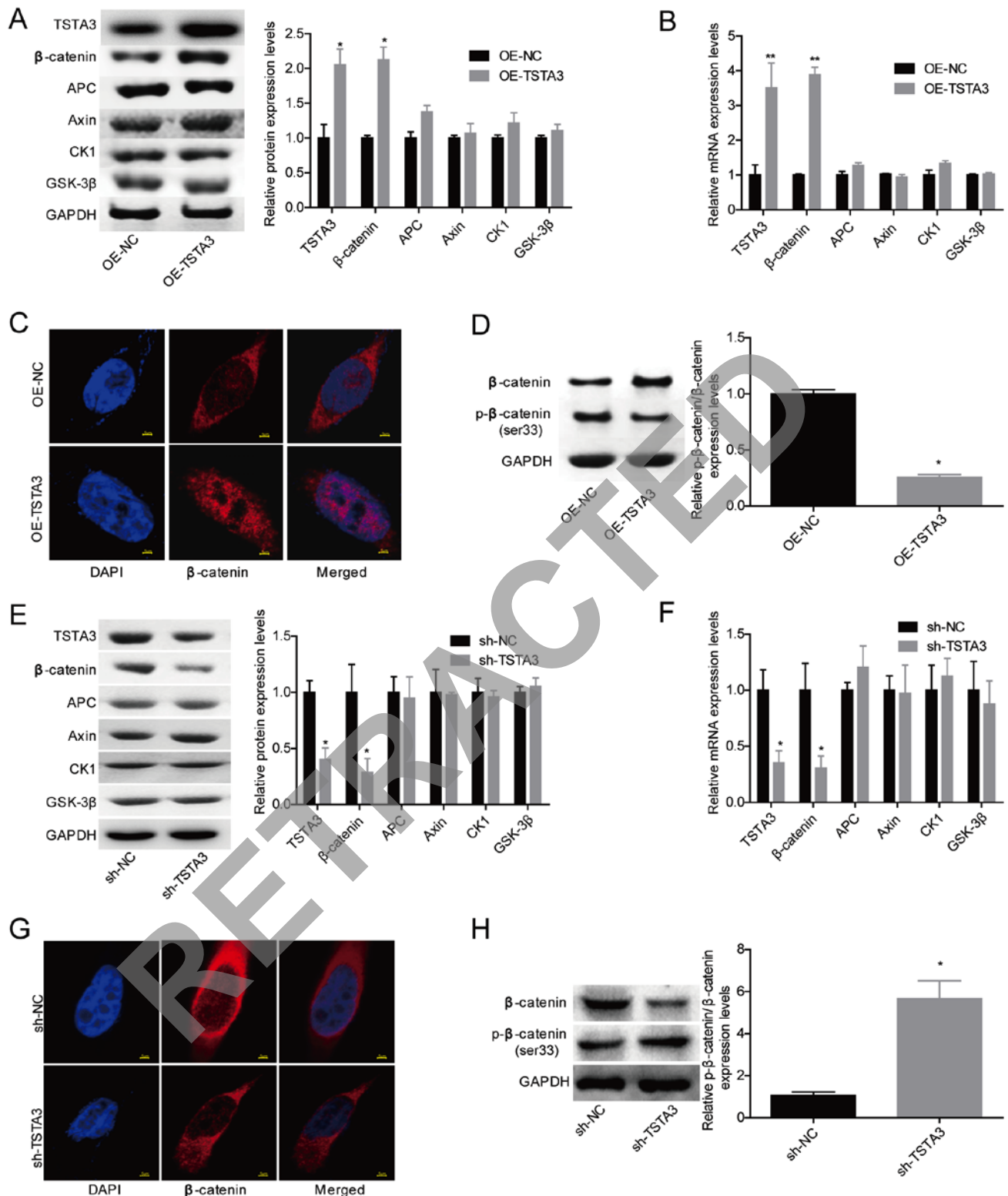


Figure 4. TSTA3 overexpression increases β-catenin expression and nuclear accumulation in NCI-H1299 cells. NCI-H1299 cells were transfected with OE-NC or OE-TSTA3, and then western blotting and RT-qPCR were used to detect the expression levels of (A) proteins and (B) mRNAs. (C) The subcellular location of β-catenin protein was assessed via immunofluorescence assay. Scale bar, 5 μm. (D) The expression levels of β-catenin and p-β-catenin were determined via western blotting. NCI-H1299 cells were transfected with sh-NC or sh-TSTA3, and then western blotting and RT-qPCR were used to detect the expression levels of (E) proteins and (F) mRNAs. (G) The subcellular location of β-catenin protein was assessed via immunofluorescence assay. Scale bar, 5 μm. (H) The expression levels of β-catenin and p-β-catenin were determined via western blotting. \*P<0.05; \*\*P<0.01 vs. OE-NC or sh-NC. NC, negative control; OE, over-expressed; sh, short hairpin; RT-qPCR, reverse transcription-quantitative PCR; TSTA3, tissue-specific transplantation antigen P35B; Axin, axis inhibitor; APC, adenomatous polyposis coil; CK1, casein kinase 1; GSK-3β, glycogen synthase kinase; p, phospho.

mRNA (Fig. 4B) levels. In addition, overexpression of TSTA3 promoted the nuclear accumulation of β-catenin (Fig. 4C)

and decreased its phosphorylation at the Ser33 site (Fig. 4D). Furthermore, knockdown of TSTA3 significantly decreased

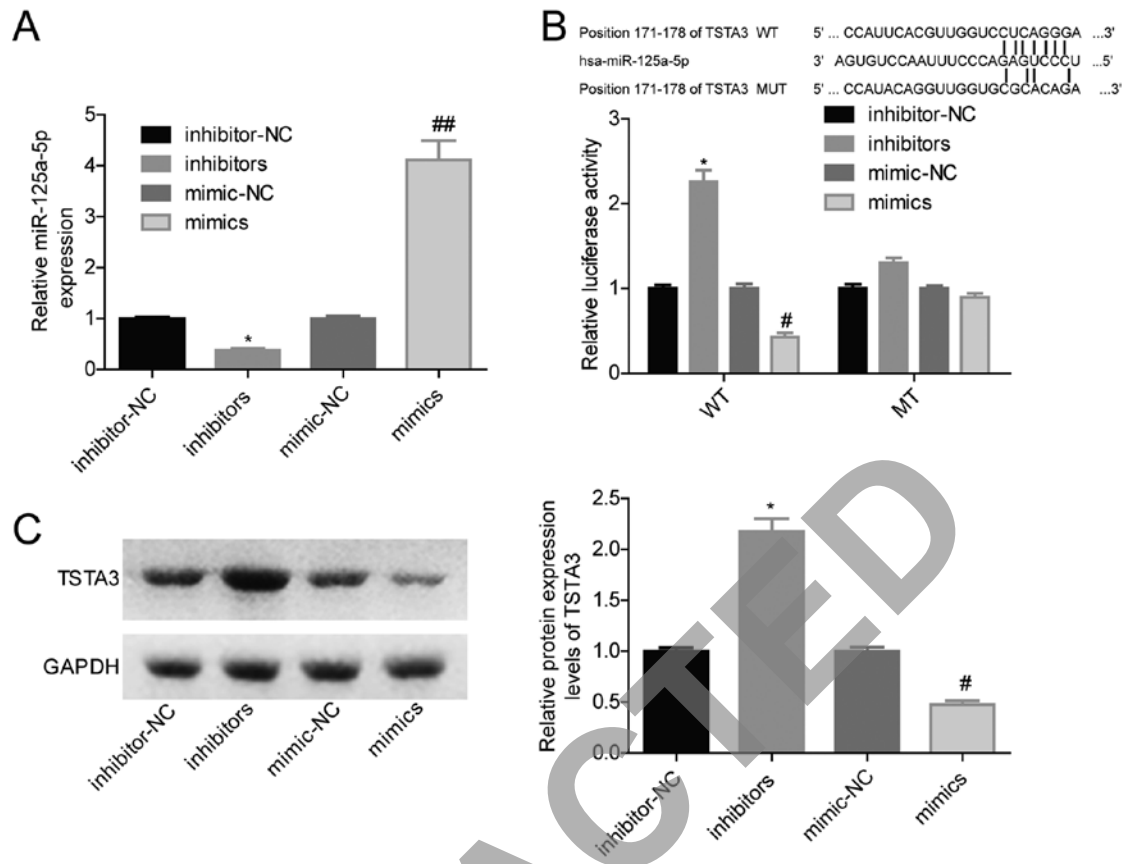


Figure 5. miR-125a-5p overexpression decreases TSTA3 expression in NCI-H1299 cells. NCI-H1299 cells were transfected with inhibitor-NC, inhibitors, mimic-NC or mimics, and then (A) miR-125a-5p expression was tested via reverse transcription-quantitative PCR. (B) Luciferase activity was determined via luciferases gene reporter assay. (C) Protein levels of TSTA3 were determined via western blotting. \* $P < 0.05$  vs. inhibitor-NC; # $P < 0.05$ , ## $P < 0.01$  vs. mimic-NC. NC, negative control; miR, microRNA, WT, wild-type; MT, mutated; TSTA3, tissue-specific transplantation antigen P35B.

$\beta$ -catenin levels (Fig. 4E and F) and nuclear content (Fig. 4G), and increased the levels of p- $\beta$ -catenin/ $\beta$ -catenin (Fig. 4H). These results suggested that TSTA3 may activate  $\beta$ -catenin signaling in lung cancer.

**miR-125a-5p negatively regulates TSTA3 expression in lung cancer cells.** To reveal the mechanisms by which TSTA3 facilitates lung cancer development, bioinformatics online softwares (TargetScan and miRDB) were used to predict the upstream regulators of TSTA3. The results demonstrated that TSTA3 expression may be regulated by miR-125a-5p. Fig. 5B shows the putative binding sites between miR-125a-5p and the 3'-UTR of TSTA3. Therefore, the effects of miR-125a-5p in TSTA3 expression were analyzed in NCI-H1299 cells. Transfection using miR-125a-5p inhibitors significantly decreased miR-125a-5p expression, while transfection with miR-125a-5p mimics significantly increased miR-125a-5p expression (Fig. 5A), compared with their respective controls. The luciferase gene reporter assay revealed that miR-125a-5p overexpression significantly decreased the luciferase activity, while knockdown of miR-125a-5p significantly increased the luciferase activity (Fig. 5B). However, miR-125a-5p modulation exhibited no significant effect on the luciferase activity when the binding sites between miR-125a-5p and TSTA3 were mutated (Fig. 5B). In addition, TSTA3 expression was significantly decreased when miR-125a-5p was overexpressed in NCI-H1299 cells and it was significantly increased when

miR-125a-5p was inhibited (Fig. 5C). These results suggested that miR-125a-5p may negatively modulate TSTA3 expression in lung cancer cells.

**Downregulation of miR-125a-5p promotes lung cancer progression via upregulating TSTA3 expression.** The roles of the miR-125a-5p/TSTA3 axis in lung cancer progression were then investigated. The results revealed that miR-125a-5p expression was significantly decreased in lung cancer tissues compared with in normal tissues (Fig. 6A). The low expression levels of miR-125a-5p were closely associated with a shorter overall survival in patients with lung cancer (Fig. 6B). The roles of miR-125a-5p/TSTA3 in lung cancer progression were then explored through *in vitro* and *in vivo* assays using HCI-H1299 cells. Knockdown of miR-125a-5p significantly increased cell proliferation (Fig. 6C) and clone formation (Fig. 6D), and decreased cell apoptosis (Fig. 6E) compared with the control, whereas these effects were weakened when TSTA3 was also inhibited (Fig. 6C-E). Furthermore, both TSTA3 overexpression and miR-125a-5p downregulation significantly increased the *in vivo* tumor formation of HCI-H1299 cells, and silencing of TSTA3 abrogated the effect of miR-125a-5p-inhibitors (Fig. 7A). In addition, the level of p- $\beta$ -catenin/ $\beta$ -catenin was decreased when TSTA3 was overexpressed or miR-125a-5p was inhibited, while TSTA3 downregulation neutralized the decrease in the expression levels of p- $\beta$ -catenin induced by miR-125a-5p-inhibitors (Fig. 7B). These results indicated that

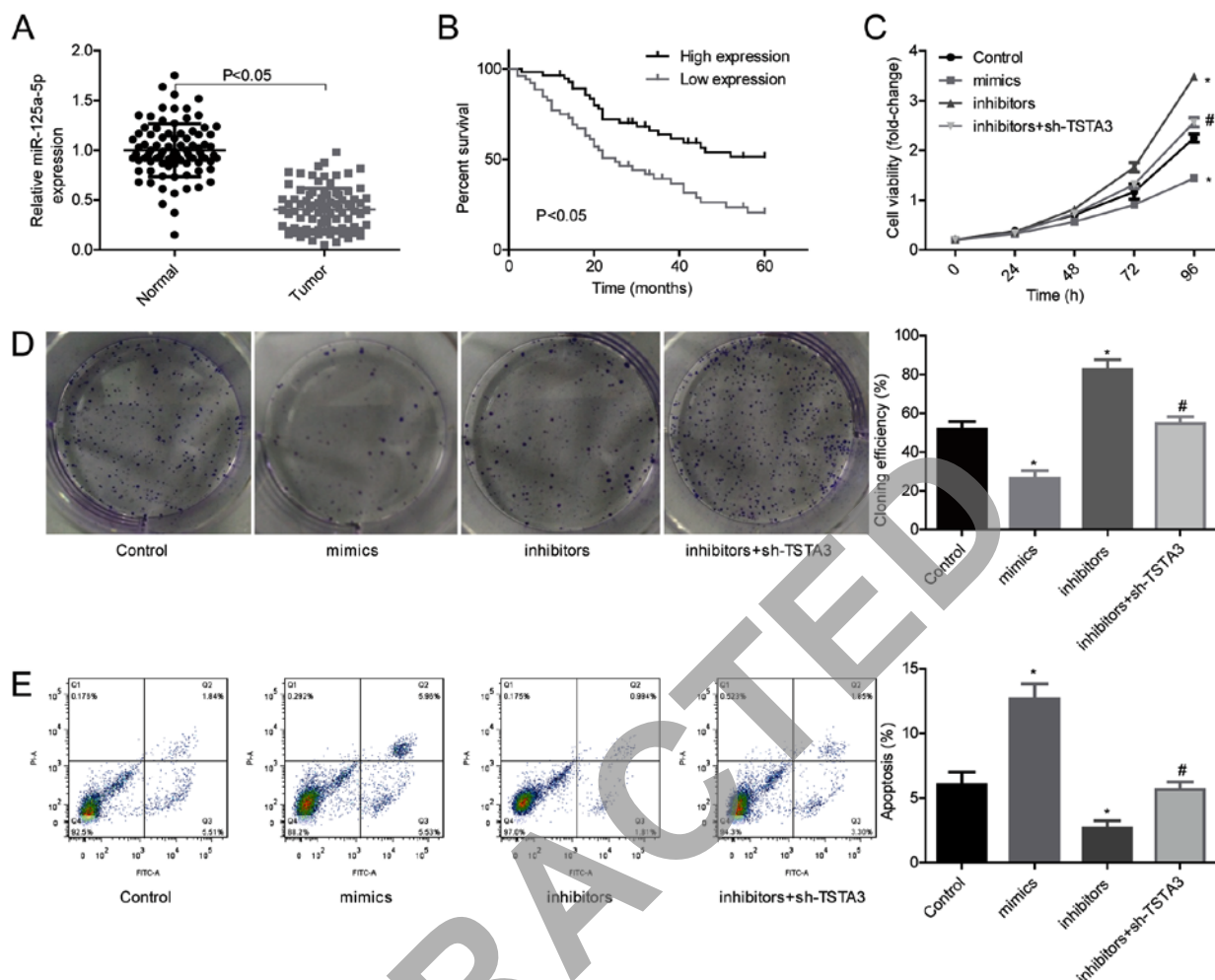


Figure 6. Roles of the miR-125a-5p/TSTA3 axis in cell proliferation, apoptosis and clone formation. (A) miR-125a-5p expression in 88 paired lung cancer and normal tissues were determined by reverse transcription-quantitative PCR. (B) Kaplan-Meier analysis was used to compare the overall survival of patients with lung cancer with high (n=49) or low (n=39) miR-125a-5p expression. After cell transfection with control vector, inhibitors, mimics or inhibitors+sh-TSTA3, NHI-H1299 cells were analyzed using (C) Cell Counting Kit-8 assay to detect cell proliferation, (D) clone formation assay to assess cell clone formation and (E) flow cytometry to assess cell apoptosis. \*P<0.05 vs. control; #P<0.05 vs. inhibitors. sh, short hairpin RNA; TSTA3, tissue-specific transplantation antigen P35B.

downregulation of miR-125a-5p may promote lung cancer progression via upregulating TSTA3 expression.

## Discussion

An increasing number of studies has illustrated that the dysregulated glycometabolism markedly contributes to the occurrence and development of lung cancer (26,27), suggesting that glycometabolism may be a target for lung cancer treatment. TSTA3 is one of the crucial enzymes modulating fucosylation and is implicated in the metabolism of mannose, and directly induces the generation of GDP-L-fucose (28). Notably, the dysregulation of GDP-L-fucose triggers the malignant transformation of cancer cells and induces malignant tumor formation in colorectal and pancreatic cancer (6,29,30). TSTA3 overexpression leads to increases in both core-fucosylated and fucosylated glycoproteins (31). Noda *et al* (32) reported that the expression levels of TSTA3, GDP-L-fucose and  $\alpha$ 1-6-fucosyltransferases were synchronously increased in hepatocellular carcinoma. Therefore, the present study hypothesized that TSTA3 may serve an important role in cancer progression. As predicted, the current

study revealed that TSTA3 expression was significantly upregulated in lung cancer tissues and cells, and that TSTA3 was negatively regulated by miR-125a-5p and functioned as an oncogene in lung cancer.

Until now, the roles of TSTA3 in predicting cancer prognosis and clinicopathological characteristics have been widely explored. For example, Yang *et al* (9) revealed that the survival rate in patients with ESCC with low TSTA3 expression is always higher than in those with high TSTA3 expression. Additionally, Sun *et al* (10) revealed that high TSTA3 expression was closely associated with a poor prognosis and an advanced TNM status (P<0.01) in patients with breast cancer. Consistently, the present study demonstrated that the expression levels of TSTA3 in lung cancer tissues were negatively associated with the overall survival and differentiation status, while they were positively associated with the TNM stage and lymph node metastasis rates in patients with lung cancer. The aforementioned findings suggest a potential value of TSTA3 as a candidate marker for cancer diagnosis and prognosis prediction.

To explore the function of TSTA3 in the progression of lung cancer, gain- and loss-of-function assays were performed. The

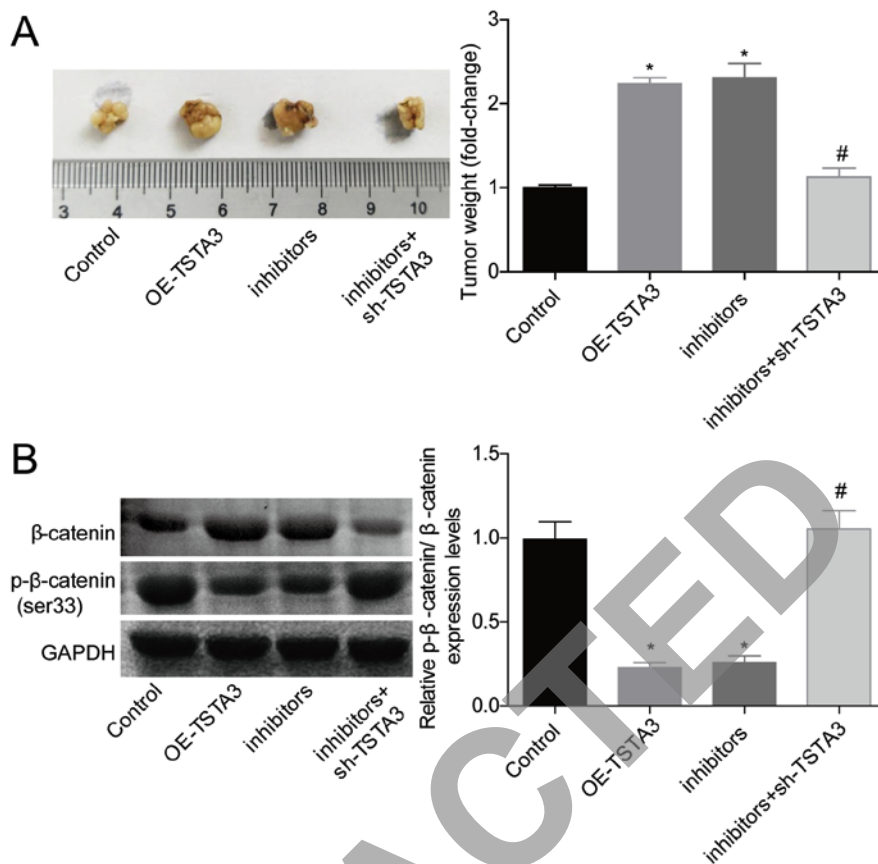


Figure 7. Assessment of the role of miR-125a-5p/TSTA3 in tumor formation from lung cancer cells. (A) Tumor-bearing experiments were performed to detect the tumorigenesis of NCI-H1299 cells in different groups: Control, OE-TSTA3, inhibitors and inhibitors+sh-TSTA3 groups. (B) The expression levels of  $\beta$ -catenin and p- $\beta$ -catenin (Ser33) in mice tumor tissues were detected via western blotting. \* $P < 0.05$  vs. control; \* $P < 0.05$  vs. inhibitors. sh, short hairpin RNA; TSTA3, tissue-specific transplantation antigen P35B; OE, overexpressed; p, phospho.

present results revealed that overexpression of TSTA3 significantly enhanced cell proliferation, clone formation, migration, invasion and tumorigenesis, and induced a significant decrease in cell apoptosis in lung cancer cells, indicating that TSTA3 may serve as an oncogene in lung cancer. The current findings were consistent with the roles of TSTA3 in breast cancer (10). However, the association between TSTA3 expression and glycosylation levels in lung cancer was not investigated in the present study, as previously reported (10).

The Wnt/ $\beta$ -catenin signaling pathway exerts an important role in the development of numerous types of cancer, including lung cancer (17). Targeting Wnt/ $\beta$ -catenin signaling is a potent method for the treatment of lung cancer (23).  $\beta$ -catenin is first phosphorylated at Ser45, Ser33, Ser37 and Thr41, and then degraded through the ubiquitin-proteasome pathway (20). Accordingly, the present study analyzed the effect of TSTA3 on the expression levels of p- $\beta$ -catenin at Ser33. It was revealed that overexpression of TSTA3 significantly decreased the expression levels of p- $\beta$ -catenin at Ser33, and increased  $\beta$ -catenin expression and its nuclear accumulation, whereas no marked changes were observed in the expression levels of APC, Axin, CK1 and GSK-3 $\beta$ , suggesting that TSTA3 activated  $\beta$ -catenin in an APC-, Axin-, CK1- or GSK-3 $\beta$ -independent manner. Future studies should further investigate this mechanism.

To reveal the molecular mechanism underlying TSTA3 in lung cancer progression, the miRNA-associated pathway

was also investigated. Bioinformatics analysis revealed that miR-125a-5p was a predicted regulator of TSTA3, which was further verified using western blotting and luciferase gene reporter assay. In addition, it was demonstrated that miR-125a-5p expression was downregulated in lung cancer, and patients with low miR-125a-5p expression had a shorter overall survival than those with high miR-125a-5p expression, which was consistent with previous studies in lung cancer (15,16). Furthermore, miR-125a-5p has been identified to exert an inhibitory role in lung cancer. Zhong *et al* (16) reported that miR-125a-5p upregulation significantly decreases the viability, proliferation and invasion of lung cancer cells, and promotes cell apoptosis via suppressing TSTA3. Naidu *et al* (33) demonstrated that miR-125a-5p enhances drug sensitivity and suppresses the invasiveness of NSCLC cells by silencing several genes involved in oncogenic KRAS and NF- $\kappa$ B signaling pathways, including SOS1, GRB2, IQGAP1, RALA, RAF-1, IKK $\beta$ , AKT2, ERK2 and KRAS itself. Similarly, the present study revealed that miR-125a-5p functioned as a tumor suppressor in lung cancer and that miR-125a-5p overexpression inhibited cell proliferation and clone formation, and induced cell apoptosis. Additionally, miR-125a-5p downregulation significantly enhanced cell proliferation, clone formation and tumorigenesis, and inhibited cell apoptosis in lung cancer cells. However, the oncogenicity induced by low miR-125a-5p expression was prevented by sh-TSTA3, indicating that

silencing of miR-125a-5p may promote lung cancer progression via increasing TSTA3 expression.

In conclusion, the present study revealed that high TSTA3 expression may predict advanced clinicopathological features and poor outcomes in patients with lung cancer. TSTA3, controlled by miR-125a-5p, may function as an oncogene in lung cancer and may induce the activation of  $\beta$ -catenin signaling. The current findings revealed the pivotal roles of the miR-125a-5p/TSTA3/ $\beta$ -catenin axis in combating lung cancer.

### Acknowledgements

Not applicable.

### Funding

No funding was received.

### Availability of data and materials

The datasets used and/or analyzed during the current study are available from the corresponding author on reasonable request.

### Authors' contributions

YG, GZ, JL and HL designed the experiments, analyzed the data and interpreted the results. YG and GZ acquired the data. YG, GZ, JL and HL wrote the manuscript and prepared the figures. JL and HL reviewed and edited the manuscript, and coordinated and directed the project. All authors read and approved the final version of the manuscript.

### Ethics approval and consent to participate

Lung cancer tissues and corresponding normal lung tissues were obtained from patients with lung carcinoma patients (60 cases were NSCLC and 28 cases were small cell lung cancer). Informed consent forms were signed by all patients. The present study involving human samples was performed in accordance with the Declaration of Helsinki and was approved by the Ethics Committee of Liaocheng People's Hospital (Liaocheng, China). The animal experiments were performed according to the National Institutes of Health Guidelines for the Care and Use of Laboratory Animals, and were approved by the Animal Care and Research Committee of Liaocheng People's Hospital.

### Patient consent for publication

Not applicable.

### Competing interests

The authors declare that they have no competing interests.

### References

- Bray F, Ferlay J, Soerjomataram I, Siegel RL, Torre LA and Jemal A: Global cancer statistics 2018: GLOBOCAN estimates of incidence and mortality worldwide for 36 cancers in 185 countries. *CA Cancer J Clin* 68: 394-424, 2018.
- Jemal A, Bray F, Center MM, Ferlay J, Ward E and Forman D: Global cancer statistics. *CA Cancer J Clin* 61: 69-90, 2011.
- Zappa C and Mousa SA: Non-small cell lung cancer: Current treatment and future advances. *Transl Lung Cancer Res* 5: 288-300, 2016.
- Siegel R, Ma J, Zou Z and Jemal A: Cancer statistics, 2014. *CA Cancer J Clin* 64: 9-29, 2014.
- Mittal V: Epithelial mesenchymal transition in aggressive lung cancers. *Adv Exp Med Biol* 890: 37-56, 2016.
- Tonetti M, Sturla L, Bisso A, Benatti U and De Flora A: Synthesis of GDP-L-fucose by the human FX protein. *J Biol Chem* 271: 27274-27279, 1996.
- Moriwaki K, Noda K, Nakagawa T, Asahi M, Yoshihara H, Taniguchi N, Hayashi N and Miyoshi E: A high expression of GDP-fucose transporter in hepatocellular carcinoma is a key factor for increases in fucosylation. *Glycobiology* 17: 1311-1320, 2007.
- Muñelo-Romay L, Villar-Portela S, Cuevas Alvarez E, Gil-Martín E and Fernández-Briera A:  $\alpha(1,6)$ Fucosyltransferase expression is an independent prognostic factor for disease-free survival in colorectal carcinoma. *Hum Pathol* 42: 1740-1750, 2011.
- Yang J, Kong P, Yang J, Jia Z, Hu X, Wang Z, Cui H, Bi Y, Qian Y, Li H, *et al*: High TSTA3 expression as a candidate biomarker for poor prognosis of patients with ESCC. *Technol Cancer Res Treat* 17: 1533033818781405, 2018.
- Sun Y, Liu X, Zhang Q, Mao X, Feng L, Su P, Chen H, Guo Y and Jin F: Oncogenic potential of TSTA3 in breast cancer and its regulation by the tumor suppressors miR-125a-5p and miR-125b. *Tumour Biol* 37: 4963-4972, 2016.
- Rotunno M, Hu N, Su H, Wang C, Goldstein AM, Bergen AW, Consonni D, Pesatori AC, Bertazzi PA, Wacholder S, *et al*: A gene expression signature from peripheral whole blood for stage I lung adenocarcinoma. *Cancer Prev Res (Phila)* 4: 1599-1608, 2011.
- Kong W, Zhao JJ, He L and Cheng JQ: Strategies for profiling microRNA expression. *J Cell Physiol* 218: 22-25, 2009.
- Kaikkonen MU, Lam MT and Glass CK: Non-coding RNAs as regulators of gene expression and epigenetics. *Cardiovasc Res* 90: 430-440, 2011.
- Janga SC and Vallabhaneni S: MicroRNAs as post-transcriptional machines and their interplay with cellular networks. *Adv Exp Med Biol* 722: 59-74, 2011.
- Liu H, Ma Y, Liu C, Li P and Yu T: Reduced miR-125a-5p level in non-small-cell lung cancer is associated with tumour progression. *Open Biol* 8: 8, 2018.
- Zhong L, Sun S, Shi J, Cao F, Han X and Chen Z: MicroRNA-125a-5p plays a role as a tumor suppressor in lung carcinoma cells by directly targeting STAT3. *Tumour Biol* 39: 1010428317697579, 2017.
- Kong X, Zhao Y, Li X, Tao Z, Hou M and Ma H: Overexpression of HIF-2 $\alpha$ -dependent NEAT1 promotes the progression of non-small cell lung cancer through miR-101-3p/SOX9/Wnt/ $\beta$ -catenin signal pathway. *Cell Physiol Biochem* 52: 368-381, 2019.
- Valenta T, Hausmann G and Basler K: The many faces and functions of  $\beta$ -catenin. *EMBO J* 31: 2714-2736, 2012.
- Sebio A, Kahn M and Lenz HJ: The potential of targeting Wnt/ $\beta$ -catenin in colon cancer. *Expert Opin Ther Targets* 18: 611-615, 2014.
- Yue B, Liu C, Sun H, Liu M, Song C, Cui R, Qiu S and Zhong M: A positive feed-forward loop between lncRNA-CYTOR and Wnt/ $\beta$ -catenin signaling promotes metastasis of colon cancer. *Mol Ther* 26: 1287-1298, 2018.
- Arce L, Yokoyama NN and Waterman ML: Diversity of LEF/TCF action in development and disease. *Oncogene* 25: 7492-7504, 2006.
- Zhang S, Li Y, Wu Y, Shi K, Bing L and Hao J: Wnt/ $\beta$ -catenin signaling pathway upregulates c-Myc expression to promote cell proliferation of P19 teratocarcinoma cells. *Anat Rec (Hoboken)* 295: 2104-2113, 2012.
- Krishnamurthy N and Kurzrock R: Targeting the Wnt/ $\beta$ -catenin pathway in cancer: Update on effectors and inhibitors. *Cancer Treat Rev* 62: 50-60, 2018.
- Woodard GA, Jones KD and Jablons DM: Lung cancer staging and prognosis. *Cancer Treat Res* 170: 47-75, 2016.
- Livak KJ and Schmittgen TD: Analysis of relative gene expression data using real-time quantitative PCR and the 2<sup>-Delta Delta</sup>CT method. *Methods* 25: 402-408, 2001.
- Taparra K, Wang H, Malek R, Lafargue A, Barbhuiya MA, Wang X, Simons BW, Balles M, Nugent K, Groves J, *et al*: O-GlcNAcylation is required for mutant KRAS-induced lung tumorigenesis. *J Clin Invest* 128: 4924-4937, 2018.

27. Shimizu M and Tanaka N: IL-8-induced O-GlcNAc modification via GLUT3 and GFAT regulates cancer stem cell-like properties in colon and lung cancer cells. *Oncogene* 38: 1520-1533, 2019.
28. Kizuka Y, Nakano M, Yamaguchi Y, Nakajima K, Oka R, Sato K, Ren CT, Hsu TL, Wong CH and Taniguchi N: An alkynyl-fucose halts hepatoma cell migration and invasion by inhibiting GDP-fucose-synthesizing enzyme FX, TSTA3. *Cell Chem Biol* 24: 1467-1478.e5, 2017.
29. Pan S, Brentnall TA and Chen R: Glycoproteins and glycoproteomics in pancreatic cancer. *World J Gastroenterol* 22: 9288-9299, 2016.
30. Villar-Portela S, Muinelo-Romay L, Cuevas E, Gil-Martín E and Fernández-Briera A: FX enzyme and GDP-L-Fuc transporter expression in colorectal cancer. *Histopathology* 63: 174-186, 2013.
31. Niittymäki J, Mattila P and Renkonen R: Differential gene expression of GDP-L-fucose-synthesizing enzymes, GDP-fucose transporter and fucosyltransferase VII. *APMIS* 114: 539-548, 2006.
32. Noda K, Miyoshi E, Gu J, Gao CX, Nakahara S, Kitada T, Honke K, Suzuki K, Yoshihara H, Yoshikawa K, *et al*: Relationship between elevated FX expression and increased production of GDP-L-fucose, a common donor substrate for fucosylation in human hepatocellular carcinoma and hepatoma cell lines. *Cancer Res* 63: 6282-6289, 2003.
33. Naidu S, Shi L, Magee P, Middleton JD, Laganá A, Sahoo S, Leong HS, Galvin M, Frese K, Dive C, *et al*: PDGFR-modulated miR-23b cluster and miR-125a-5p suppress lung tumorigenesis by targeting multiple components of KRAS and NF-κB pathways. *Sci Rep* 7: 15441, 2017.



This work is licensed under a Creative Commons Attribution-NonCommercial-NoDerivatives 4.0 International (CC BY-NC-ND 4.0) License.

RETRACTED